



Acid Gas, Acid Aerosol and Chlorine Emissions from Trichlorosilane Burning Processes

Jhy-Charm Soo¹, Siou-Rong Li¹, Jenq-Renn Chen², Cheng-Ping Chang³, Yu-Fang Ho³,
Trong-Neng Wu^{4*}, Perng-Jy Tsai^{1,4*}

¹ Department of Environmental and Occupational Health, Medical College, National Cheng Kung University, 138, Sheng-Li Road, Tainan 70428, Taiwan

² Department of Safety, Health and Environmental Engineering, National Kaohsiung First University of Science & Technology, University Road, Yenchau, Kaohsiung, 824, Taiwan

³ Institute of Occupational Safety and Health, Council of Labor Affairs, 99, Lane 407, Hengke Road, Sijhih City, Taipei County 22143, Taiwan

⁴ Department of Occupational Safety and Health, College of Public Health, China Medical University and Hospital, 91, Hsueh-Shih Road, Taichung 40402, Taiwan

ABSTRACT

This study was set out to investigate the emission characteristics of HCl (in both particle (HCl_p) and gaseous (HCl_g) forms), and Cl₂ during the trichlorosilane (TCS) burning process under various relative humidity conditions (RH; range = 55%–90%) which might exist at its storage area. All experiments were conducted in a test chamber. We found that HCl_p was consistently as the most dominant contaminant ($= 1.30 \times 10^5$ – 1.46×10^5 mg/m³), followed by the HCl_g ($= 9.03 \times 10^3$ – 11.4×10^3 mg/m³) and Cl₂ ($= 1.91 \times 10^3$ – 2.18×10^3), emitted from the TCS burning process for the all selected RH conditions. The particle sizes of HCl_p fell to the range of the accumulation mode (MMADs = 0.808–1.04 μm; GSDs = 2.13–3.50). Fractions of emitted HCl_p reaching to the alveolar region ($= 85.8$ – 88.8%) were much higher than that of the tracheobronchial region ($= 6.53$ – 8.80%) and head region ($= 4.67$ – 5.40%). It is concluded that more ill-health effects on the deep lung region can be expected than other regions as workers exposed to the contaminants emitted from TCS burning processes.

Keywords: Trichlorosilane; Burning process; Acid gas, Acid aerosol; Chlorine.

INTRODUCTION

According to statistical data, the annual world production of trichlorosilane (TCS) is ~350,000–380,000 tons and ~60–65% of TCS is consumed by the semiconductor industry as an alternative silicon source gas (Howe-Grant, 1997; Williams, 2000). TCS is also used as the basic ingredient in the production of solar cells, optical fibers, and the manufacturing of PV grade polysilicon and silane gas. For the above industries, many study have been conducted to address their fugitive emissions at process areas (Hu *et al.*, 2010; Lin *et al.*, 2010; Shih *et al.*, 2010) or pollutant removal

efficiencies of various air pollution control devices (Lin *et al.*, 2010; Shiue *et al.*, 2011). Though many studies have been conducted to address the emissions arising from combustion related activities (Choosong *et al.*, 2010; Li *et al.*, 2010; Ning *et al.*, 2010), very limited have been conducted to characterize the emissions of raw materials during the accidental fire or explosion cases.

TCS is known with a boiling point of 31.85°C, flash point of –28°C, and flammability range of 7%–82% (Laurence, 1990). Apparently, its major hazard might simply lie on its flammability. Therefore, TCS emergency response guidelines proposed by different organizations, such as the Silicones Environmental, Health and Safety Council of North America (SEHSC), Centre Européen des Silicones (CES), Silicone Industry Association of Japan (SIJA), concern still mostly on its fire and explosion effects, rather on the impact caused by its resultant combustion by-products (e.g., hydrogen chloride (HCl) and chlorine (Cl₂)) (Higgins *et al.*, 1999; CES, 2003). However, the impact of its combustion by-products has never been investigated.

* Correspondence author. Tel.: +886-6-2353535 ext. 5806;
Fax: +886-6-2752484
E-mail address: pjtsai@mail.ncku.edu.tw;
or Tel.: +886-4-22053366 ext. 1000;
Fax: +886-4-22060648
E-mail address: tnwu@mail.cmu.edu.tw

In principle, the generation of HCl from the TCS burning process can be described as (Mores, 1984):



In addition, part of emitted Cl_2 could further react with H_2O to form HCl:



From the Eq. (1), the generated HCl could be presented simultaneously in both gaseous (i.e., HCl_g) and aerosol (i.e., HCl_p) forms. Here, HCl_p might be formed directly via the condensation of HCl_g on particles (such as SiO_2) via the heterogeneous condensation process, or by directly dissolving HCl_g into H_2O coated on the surface of SiO_2 particle or water droplets. From Eq. (2), the generated HCl might directly dissolve water droplets to form HCl_p .

Among these emitted contaminants, Cl_2 is known for its acute health effect on the respiratory system (Agabiti *et al.*, 2001; Rabinowitz and Siegel, 2002; Uyan *et al.*, 2009) and acute ischemic stroke (Kose *et al.*, 2009). HCl_g is an upper respiratory tract irritant because of its high water-solubility

(Salem, 2005). HCl_p , on the other hand, might penetrate into the deep lung of the respiratory tract and cause more serious ill-health effects depending on its particle size (ICRP, 1994). Therefore, simultaneously measuring Cl_2 , HCl_g and HCl_p are considered a better approach to characterize the release of toxic chemicals from the TCS burning process.

In this study, a chamber study was conducted to investigate the emission characteristics of Cl_2 , HCl_g and HCl_p during the TCS combustion process. In order to simulate the real situation for TCS storage in the indoor gas yard, four relative humidity (RH) conditions were used based on RH records provided by semiconductor industries in Taiwan. The results obtained from this research will provide information for the government, semiconductor and optoelectronic industries to generate appropriate strategies for TCS emergency response process.

MATERIAL AND METHODS

Test Chamber and its Apparatus

Fig. 1 shows the stainless steel 316 test chamber used in the present study. The chamber comprised three parts,

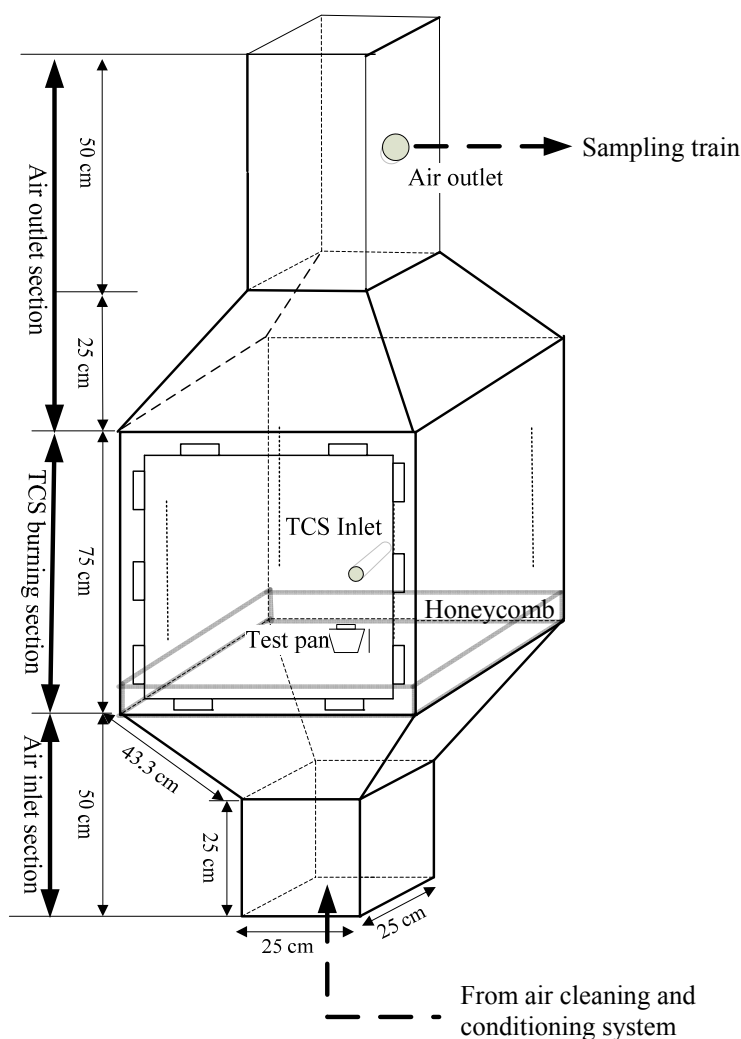


Fig. 1. Schematic of the test chamber used in this study.

including an air inlet section (i.e., the lower pyramid part), a TCS burning section, and an air outlet section (i.e., the upper pyramid part). Before the supply air entering into the lower pyramid, it was treated by an air cleaning and conditioning system (Fig. 2). The system consisted of a compressor, a dryer, a surge tank, an activated charcoal, a high-efficiency particulate air (HEPA) filter, a home-made heating tank, and a humidifier (model FC-125, Perma Pure Inc., NJ, USA). The mass flow controller (MFC, Side-Trak® Model 840, Sierra Instruments Inc., CA, USA) was also installed in the system to ensure to provide a designated air flow with a preset humidity condition. The flat top of the air inlet section was installed with a honeycomb to provide a uniformly distributed laminar flow for the TCS burning section. This burning section was a 0.42 m³ cube installed with one glass door, and three stainless steel side-walls. On the opposite wall of the glass door was installed with a TCS feeding tube (diameter = 0.64 cm) to transport a fixed amount of TCS (ACS grade, ~99.9% purity) from the TCS storage cylinder to the test pan (diameter = 5.0 cm, height = 3.0 cm). In order to know the consumption rate of TCS, the test pan was placed on a digital balance (accuracy = ± 0.02 g, model SKY-600, Javeder Scale Co., Taiwan) to continuously send weight signals to the laptop per 1/30,000 second during each combustion test run. All air samples were collected at the converging part of the air outlet section.

Selected Test Conditions

Four RH conditions (= 55%, 65%, 80% and 90%) were selected for conducting TCS combustion experiments to simulate possible humidity conditions of the storage area year round. After being pretreated by the air cleaning and conditioning system, the RH conditions used in the present study were 57.3%, 65.5%, 79.8% and 89.8%, respectively (with relative standard deviations (RSDs) < 1.01%). The air flow feeding rate was specified at 0.042 m³/min by a mass flow controller in the present study to simulate the air change per hour (ACH = 6) commonly found in the indoor gas yard. The resultant chamber air velocity (0.0017 m/s)

was also comparable to the indoor work environment. To assess the uniformity of air velocities occurred at the TCS burning section, four cross-sections were chosen from the length of the burning section. For each cross-section, it was divided into 16 equal areas (~0.035 m² for each area) and air velocities measurements were conducted at the center of each area. The total measured air velocities were ranging from 0.0017 to 0.0019 m/s (RSD = 1.20%) indicating the uniformity of the test chamber was quite acceptable.

Sample Collection and Analysis

For each selected test conditions, three repeated particle size segregating samplings were conducted at the converging part of the air outlet section of the test chamber using a Micro-Orifice Uniform Deposit Impactor (MOUDI™ model 110, MSP Corp., Minneapolis, MN, USA), and followed by Nano Micro-Orifice Uniform Deposit Impactor (Nano-MOUDI™ model 115, MSP Corp., Minneapolis, MN, USA) for collecting the generated HCl_p. The whole sampling train consisted of an inlet stage (with a 50% cut-off aerodynamic diameter ($d_{50\%}$) of 18 μm), thirteen impaction stages (with $d_{50\%}$ s of 10.0, 5.6, 3.2, 1.8, 1.00, 0.56, 0.32, 0.18, 0.10, 0.056, 0.032, 0.018, and 0.010 μm, respectively), and a 37 mm PTFE back-up filter (pore size = 2.0 μm, Zeflour™ Pall Corp., Ann Arbor, MI, USA). The summation of HCl_p concentrations of all impaction stage and the back-up filter was regarded as the total HCl_p concentration. The sampling flow rates of MOUDI™ and Nano-MOUDI™ were set at 30.0 and 10.0 L/min, respectively and were checked periodically throughout the entire sampling period. Yet, it is true that many instruments can be used to conduct aerosol samplings with particle sizes covering both micron and submicron ranges (Li *et al.*, 2009; Kim *et al.*, 2010; Liu *et al.*, 2010; Intra *et al.*, 2011), the use of MOUDI and Nano-MOUDI in the present study has the advantage in their continuous collected particle size ranges.

Beside HCl_p, three repeated HCl_g and Cl₂ samples were simultaneously collected using a silica gel tube (Cat. No. 226-10-03, SKC Inc., Eighty Four, PA, USA) and a 25 mm sliver membrane filter (pore size = 0.45 μm, Cat. No. 225-

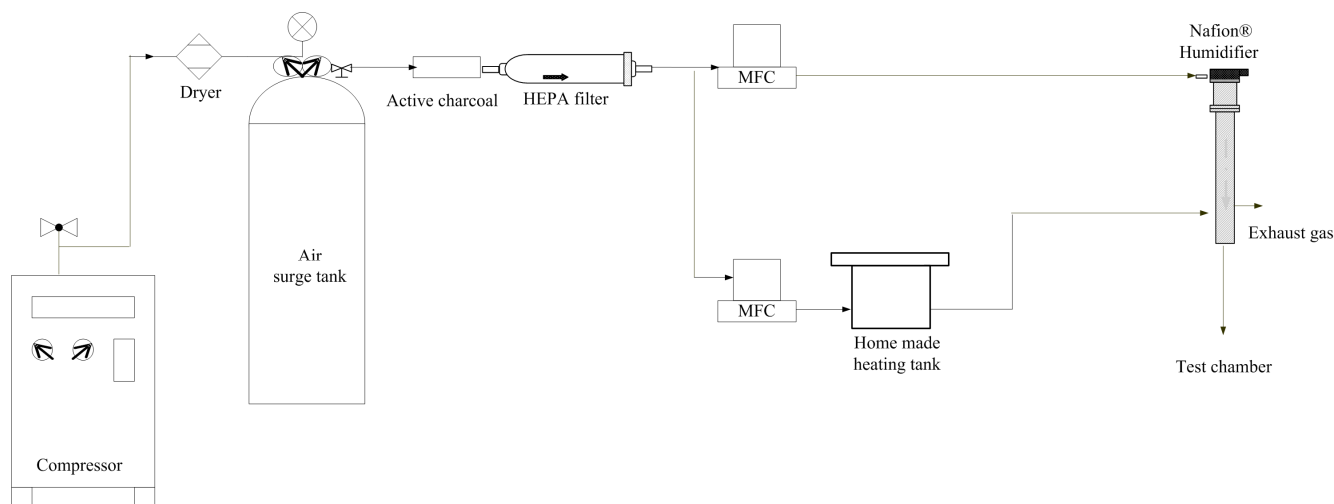


Fig. 2. Schematic of the air cleaning and conditioning system used in this study.

1802, SKC Inc., Eighty Four, PA, USA) per the NIOSH method 7903 and 6011, respectively. Both sampling flow rates were specified at 0.3 L/min and were also checked periodically throughout the entire sampling period.

All collected HCl_p, HCl_g and Cl₂ samples were analyzed by using the Ion Chromatography with Electron Capture Detection (DX-100 model, Dionex Corp., Sunnyvale, CA). This study yields method of detection limit (MDL) of 3.09 µg/µL for chloride (Cl⁻).

Data Analysis

In this study, the descriptive statistics was used to describe the concentrations of HCl_p, HCl_g and Cl₂ (i.e., C_{HClp}, C_{HClg}, and C_{Cl2}) obtained from the four selected RH conditions. The differences among the above resultant concentrations were examined by using the Kruskal-Wallis test. For each test condition, the particle size distribution was obtained by averaging the three collected size-segregating samples. Both the mass median aerodynamic diameter (MMAD) and geometric standard deviation (GSD) was used to describe the resultant particle size distribution. Here, GSD can be estimated either by $d_{50\%}/d_{16\%}$ or $d_{84\%}/d_{50\%}$, where $d_{n\%}$ represents the aerodynamic diameter at d_{ac} with a $n\%$ cumulative fraction for the given particle size distribution (Ramachandran, 2005). The resultant size distribution data was further used to estimate mass concentrations of the inhalable (C_{inh}), thoracic (C_{thor}), and respirable (C_{resp}) fractions of C_{HClp} based on the three particle size-selective sampling conventions adopted by the International Standards Organization (ISO), the Comité Européen Normalization (CEN), and American Conference of Governmental Industrial Hygienists (ACGIH) (ISO, 1995; CEN, 1993; ACGIH, 1984). Here, inhalable, thoracic, and respirable aerosols represent the fraction of particles which is aspirated through the nose and /or mouth during breathing, the fraction of inhaled particles which passes into the lung below the larynx, and the fraction of inhaled particles which passes down to the alveolar (or gas exchanging) region of the lung, respectively. Based on the above definitions, the concentrations of HCl_p reaching the head region (C_{head} = C_{inh} - C_{thor}), tracheobronchial region (C_{tb} = C_{thor} - C_{resp}), and alveolar region (C_{alv} = C_{resp}) under the four selected RH conditions could be estimated (Tsai et al., 1995, 1996; Vincent, 2005; Chen et al., 2007; Chen et al., 2007; Shih et al., 2009). In addition, fractions of inhaled HCl_p reaching the head region ($F_{head} = C_{head}/C_{inh}$), tracheobronchial region ($F_{tb} = C_{tb}/C_{inh}$), and alveolar region ($F_{alv} = C_{alv}/C_{inh}$) were also determined.

RESULTS AND DISCUSSION

C_{HClp}, C_{HClg}, and C_{Cl2} Emitted from TCS Burning Processes

Table 1 shows means and their corresponding RSDs of C_{HClp}, C_{HClg}, and C_{Cl2} emitted from TCS burning processes under the four selected RH conditions. For all test conditions, we found that the C_{HClp} (mean = 1.30×10^5 – 1.46×10^5 mg/m³; RSD = 6.90–22.0%) was the most dominant by-product, followed by the C_{HClg} (mean = 9.03×10^3 – 11.4×10^3 mg/m³; RSD = 8.90–37.1%) and C_{Cl2} (mean = 1.91×10^3 – 2.18×10^3 mg/m³; RSD = 4.00–11.0%). Here, it should be noted that no significant difference was found among C_{HClp} obtained from the four selected RH conditions (Kruskal-Wallis test, $p > 0.05$). The same trend can also be seen in C_{HClg} and C_{Cl2}. The above results indicate that RH didn't have a significant effect on the composition of the by-products emitted from the TCS burning process.

The emitted HCl concentrations (i.e., C_{HClp} + C_{HClg}) were much higher than Cl₂ concentrations (i.e., C_{Cl2}). Apparently, it was contradictory to the theoretical predictions based on eq. (1) (i.e., C_{Cl2} should be ~14 times in magnitude higher than that of the summation of C_{HClp} and C_{HClg}). The above inconsistency might be explained by Eq. (2) (i.e., most of the generated Cl₂ might further react with H₂O to form HCl). The above inference is consistent with results found by Chow et al. (1994). They found that ~90% of chloride containing in the coal was converted to HCl during the coal combustion process. Therefore, it could be concluded that the existence of water vapor during TCS burning process would result in less acute inhalatory effect because of converting the emitted Cl₂ into HCl_p. However, more serious deep lung irritation and inflammation might occur due to higher resultant concentrations in HCl_p. In the present study, we also found that C_{HClp} was much higher than that of C_{HClg}. The above result was not so surprising because (1) the generated HCl_g might condensate on existing SiO₂ particles to form HCl_p via the heterogeneous condensation process (Friedlander, 2000), (2) the generated HCl_g might dissolve into H₂O coated on the surface of SiO₂ particle, and (3) the generated Cl₂ might further react with H₂O to form HCl_p.

Finally, our study also indicated that humidity didn't have a significant effect on the compositions of TCS burning products. By examining all test conditions, ~0.655–0.962 g/min humidity was originally containing in the inlet air (RH = 57.3–89.8 %). In addition, there was ~0.440–0.498 g/min water vapor emitted from TCS burning processes based on the TCS consumption rates (CR = 8.28–9.38 g/min) obtained from this study.

Table 1. Mean emitted concentrations of C_{HClp}, C_{HClg}, and C_{Cl2} and their corresponding relative standard deviations (RSDs) from TCS burning processes under the four selected RH conditions

RH (%)	C _{HClp}		C _{HClg}		C _{Cl2}	
	Mean (mg/m ³)	RSD (%)	Mean (mg/m ³)	RSD (%)	Mean (mg/m ³)	RSD (%)
57.3	1.35×10^5	22.0	10.6×10^3	8.90	2.05×10^3	11.0
65.5	1.46×10^5	6.90	11.3×10^3	20.2	1.91×10^3	10.1
79.8	1.43×10^5	11.7	9.52×10^3	9.70	2.18×10^3	7.20
89.8	1.30×10^5	10.2	9.03×10^3	37.1	2.11×10^3	4.00

Theoretically, the required water vapor importing rate to maintain the saturation condition of the test chamber was 1.07 g/min (at 25°C). Considering the total water vapor importing rates (i.e., water vapor containing in the inlet air + water vapor emitted from the TCS burning process) (= 1.12–1.46 g/min) were consistently higher than 1.07 g/min indicating that the test chamber was always on a water saturated condition for all TCS burning experiments. As a result, the effect of humidity on the compositions of TCS burning products becomes insignificant.

Particle Size Distributions of HCl_p

Table 2 shows particle size distributions of HCl_p obtained from the four selected RH conditions. It can be seen that the emitted particles (MMADs = 0.808–1.04 μm ; GSDs = 2.13–3.50) fell to the range of the accumulation mode (0.1–2.5 μm). For illustration, Fig. 3 shows the particle size distribution obtained from the test condition of RH = 65.5%. As described in the previous section, HCl_p could be generated by condensation of HCl_g on the emitted SiO_2 particles via the heterogeneous condensation process, or via the absorption of HCl_g onto H_2O coated on SiO_2 particle surface. Based on the above description, the emitted HCl_p particles might fall to the range of the nuclei mode (i.e., 0.1 μm). However, it should be noted that the

particle sizes of these primary HCl_p particles might further increase to the accumulation mode because of the effects caused by both the Brownian and turbulent coagulation (Friedlander, 2000). In addition, our results were also consistent with the results obtained by Schenkel and Schaber (1995).

Yet, it is true that high moisture content in the air might lead to an increase in the particle size according to the Kelvin effect theorem (Friedlander, 2000; Hu *et al.*, 2010). In this study, the four selected RH conditions did not affect the emitted particle sizes of HCl_p which might because the test chamber was always on a water saturated condition for all TCS burning experiments (as described earlier).

Fractions of Inhaled HCl_p Reaching Different Regions of the Respiratory Tract

Fig. 4 shows the fractions of inhaled HCl_p reaching the alveolar region (F_{alv}), tracheobronchial region (F_{tb}), and head region (F_{head}) under the four selected RH conditions during the TCS burning process. For all test conditions, a consistent trend of F_{alv} (mean = 85.8–88.8 %; RSD = 1.50–7.45 %) > F_{tb} (mean = 6.53–8.80 %; RSD = 0.50–4.90 %) > F_{head} (mean = 4.67–5.40 %; RSD = 0.60–2.62 %) was found in the present study. The highest fraction found in the alveolar region indicates that most HCl_p emitted from

Table 2. Particle size distribution of HCl_p emitted from TCS burning processes under the four selected RH conditions.

RH (%)	Particle size distributions of HCl_p	
	MMAD (μm)	GSD
57.3	0.939	2.13
65.5	1.04	3.43
79.8	0.861	3.50
89.8	0.808	3.49

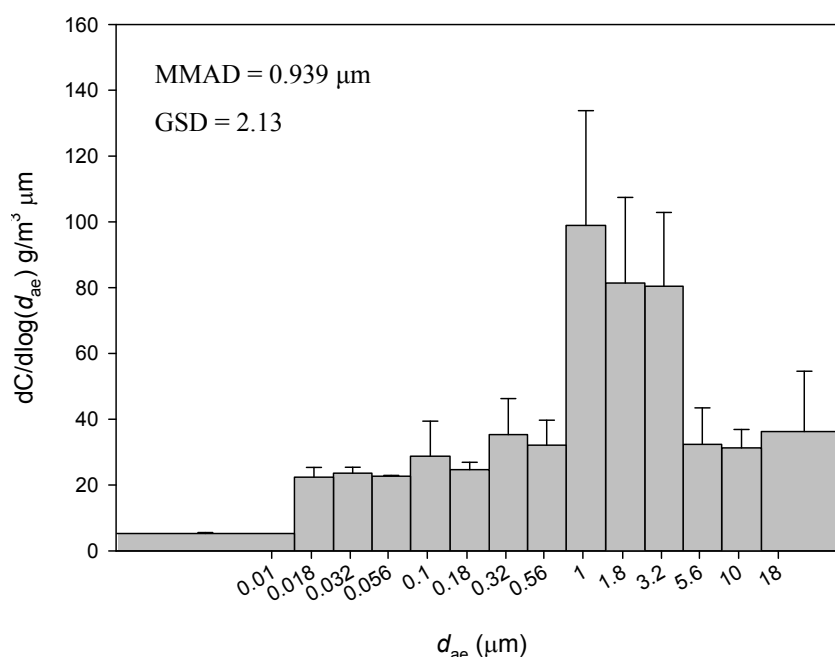


Fig. 3. The particle size distribution of HCl_p emitted from the during the TCS burning process under the test condition of RH = 65.5 %

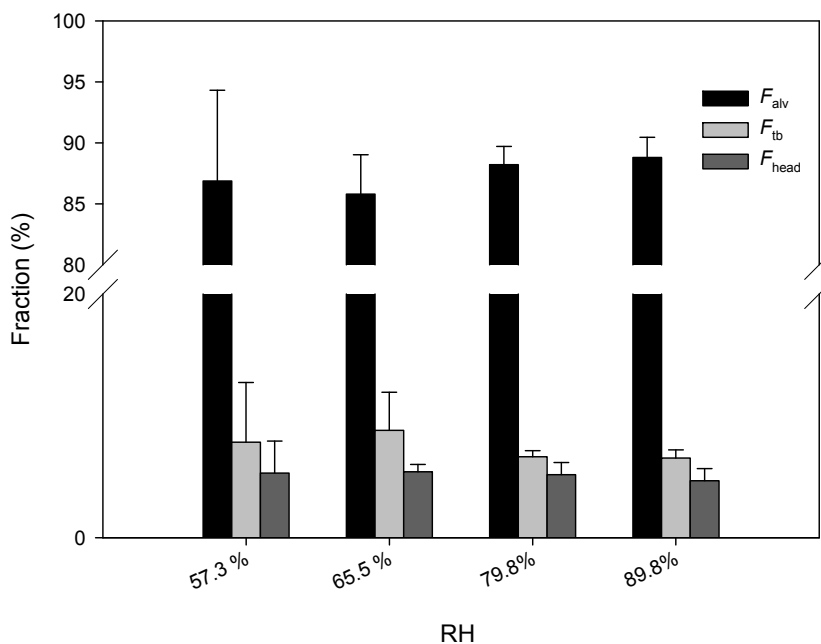


Fig. 4. Estimated fractions of inhaled HCl_p reaching the head region (F_{head}), tracheobronchial region (F_{tb}), and alveolar region (F_{alv}) during the TCS burning processes under the four selected RH conditions.

TCS burning processes could penetrate into the deep lung of the respiratory tract. It is known that HCl_g could only reach the upper respiratory tract due to its high water solubility. In particular, as described in the previous section, the emitted C_{HCl_p} ($= 1.30 \times 10^5$ – 1.46×10^5 mg/m³) were consistently much higher than C_{HCl_g} ($= 9.03 \times 10^3$ – 11.4×10^3 mg/m³) in all experimental campaigns. Our results suggest more serious damage might occur at the deep lung region than other regions of the respiratory tract as workers exposed to contaminants emitted from TCS burning processes.

Theoretical and Measured Total Chloride Emitted Concentrations

Table 3 shows the consumption rates of TCS and the measured total chloride emitted concentrations and their corresponding theoretical values under the four selected RH conditions. No significant difference can be found in consumption rates of TCS among the four selected RH conditions (mean = 8.28–9.39 g/min; RSD = 6.56–19.0 %) (Kruskal-Wallis test, $p > 0.05$). Therefore, it could be expected that no significant difference can be found in the theoretical total chloride emitted concentrations (mean =

1.55×10^5 – 1.75×10^5 g/min; RSD = 6.56–19.0 %) (Kruskal-Wallis test, $p > 0.05$). On the other hand, we found that there were slight differences between theoretical and their corresponding measured total chloride emitted concentrations (mean = 1.40×10^5 – 1.60×10^5 mg/m³; RSD = 8.19–26.1%). Based on the above values, the resultant recoveries ($= (\text{measured values}/\text{theoretical values}) \times 100\%$) fell to the range of 90.1–91.0 %. The above discrepancies were because the parts of HCl were not sampled in the present study, including those were deposited on the chamber walls, or being absorbed by the H₂O coated on the chamber wall. However, the above results also suggest that our results can fairly characterize the emissions of contaminants from the TCS burning processes.

CONCLUSIONS

We found that the HCl_p was consistently as the most dominant contaminant, followed by the HCl_g and Cl₂, emitted from the TCS burning processes. We also found that humidity didn't have a significant effect on the composition of the above three emitted contaminants under the four RH test conditions. Therefore, lower RH test

Table 3. Comparisons of theoretical total chloride emitted concentrations with their corresponding measured values under the four selected RH conditions.

RH (%)	TCS consumption rate		Total chloride emitted concentrations				
			Theoretical concentrations		Measured concentrations		Recovery (%)
Mean (g/min)	RSD (%)	Mean (mg/m ³)	RSD (%)	Mean (mg/m ³)	RSD (%)		
57.3	8.73	19.0	1.64×10^5	19.0	1.4×10^5	26.1	90.5
65.5	9.39	6.56	1.76×10^3	6.56	1.60×10^5	9.06	91.0
79.8	9.11	12.0	1.71×10^3	12.0	1.54×10^5	8.19	90.1
89.8	8.28	11.64	1.55×10^3	11.6	1.40×10^5	14.1	90.2

conditions are suggested for further research in the future, in particular for TCS could be stored in areas with much lower RH conditions. The emitted HCl_p fell to the range of the accumulation mode, and the fraction of HCl_p deposited on the alveolar region was consistently higher than those on the tracheobronchial region and head region for the selected RH test range. Therefore, more serious ill-health effect on the deep lung region of the respiratory tract can be expected as workers exposed to contaminants emitted from TCS burning processes. The results obtained from this study will provide information for semiconductor and optoelectronic industries to initiate an appropriate TCS emergency response plan to prevent workers from the ill-health effects associated with toxics emitted from TCS burning processes.

ACKNOWLEDGEMENT

The authors wish to thank the Institute of Occupational Safety and Health (IOSH) of the Council of Labor Affairs in Taiwan for funding this research project.

REFERENCES

- ACGIH (1984). *ACGIH Technical Committee on Air Sampling Procedures: Particle Size-selective Sampling in the Workplace*, American Conference of Governmental Industrial Hygienists, Ohio, USA.
- Agabiti, N., Ancona, C., Forastiere, F., Napoli, A.D., Presti, E.L., Corbo, G.M., D'Orsi, F. and Perucci, C.A. (2001) Short Term Respiratory Effects of Acute Exposure to Chlorine Due to a Swimming Pool Accident. *Occup. Environ. Med.* 58: 399–404.
- CEN (1993). *Workplace Atmospheres: Size Fraction Definitions for Measurement of Airborne Particles in the Workplace*, Comité Européen de Normalisation standard EN 481, Belgium.
- CES (2003). *Safe Handling of Chlorosilanes*, Centre Européen des Silicoles, Bressuls, Belgium.
- Chen, J.L., Su, L.F., Tsai, C.L., Liu, H.H., Lin, M.H., Tsai, P.J. (2007). Mass, Number and Surface Area Concentrations of α -Quartz Exposures of Refractory Material Manufacturing Workers. *J. Occup. Health* 49: 411–417.
- Chen, M.R., Tsai, P.J., Chang, C.C., Shih, T.S., Lee, W.J. and Liao, P.C. (2007). Particle Size Distributions of Oil Mists in Workplace Atmospheres and Their Exposure Concentrations to Workers in a Fastener Manufacturing Industry. *J. Hazard. Mater.* 146: 393–398.
- Choosong, T., Chomane, J., Tekasakul, P., Tekasakul, S., Otani, Y., Hata, M. and Furuuchi, M. (2010). Workplace Environment and Personal Exposure of PM and PAHs to Workers in Natural Rubber Sheet Factories Contaminated by Wood Burning Smoke. *Aerosol Air Qual. Res.* 10: 8–21.
- Chow, W., Miller, M.J. and Torrens, I.M. (1994) Pathways of Trace-elements in Power-plant Interim Research Results and Implications. *Fuel Process. Technol.* 39: 5–20.
- Friedlander, S.K. (2000). *Smoke, Dust, and Haze: Fundamentals of Aerosol Dynamics*, 2nd ed., Oxford University Press, New York.
- Higgins, J. T., Kayser, R. A., Kremer, P., McMahan, S. W., Patrick, L., and Strong, M. (1999). *Manual on Chlorosilane Emergency Response Guidelines*, ASTM MNL 33, USA.
- Howe-Grant, M.K. (1997). *Kirk-Othmer Encyclopedia of Chemical Technology*, John Wiley & Sons, New York, USA.
- Hu, D., Qiao, L., Chen, J., Ye, X., Yang, X., Cheng, T. and Fang, W. (2010). Hygroscopicity of Inorganic Aerosols: Size and Relative Humidity Effects on the Growth Factor. *Aerosol Air Qual. Res.* 10: 255–264.
- ICRP (1994). Human Respiratory Tract Model for Radiological Protection, In *Publication 66, Annals of ICRP*, Pergamon, London, UK.
- Intra, P. and Tippayawong, N. (2011). An Overview of Unipolar Charger Developments for Nanoparticle Charging. *Aerosol Air Qual. Res.* 11: 187–209.
- ISO (1995). *Air Quality – Particle Size fraction Definitions for Health-related Sampling 7708*, International Organization for Standardization, Geneva, Swiss.
- Kim, K.H., Sekiguchi, K., Kudo, S., Sakamoto, K., Hata, M., Furuuchi, M., Otani, Y. and Tajima N. (2010). Performance Test of an Inertial Fibrous Filter for Ultrafine Particle Collection and the Possible Sulfate Loss when Using an Aluminum Substrate with Ultrasonic Extraction of Ionic Compounds. *Aerosol Air Qual. Res.* 10: 616–623.
- Kose, A., Kose, B., Acikalin, A., Gunay, N. and Yildirim, C. (2009). Myocardial Infarction, Acute Ischemic Stroke, and Hyperglycemia Triggered by Acute Chlorine Gas Inhalation. *Am. J. Emergency Med.* 27: 1022–1022.
- Laurence, G.B. (1990). Combustion Hazards of Silane and Its Chlorides. *Plant/Oper. Prog.* 9: 16–38.
- Li, H., Han, Z., Cheng, T., Du, H., Kong, L., Chen, J., Zhang, R. and Wang, W. (2010). Agricultural Fire Impacts on the Air Quality of Shanghai during Summer Harvesttime. *Aerosol Air Qual. Res.* 10: 95–101.
- Li, L., Chen, D.R. and Tsai, P.J. (2009). Use of An Electrical Aerosol Detector (EAD) for Nanoparticle Size Distribution Measurement. *J. Nanopart. Res.* 11: 111–120.
- Lin, I.K., Bai, H. and Wu, B.J. (2010). Analysis of Relationship between Inorganic Gases and Fine Particles in Cleanroom Environment. *Aerosol Air Qual. Res.* 10: 245–254.
- Lin, T., Tung, Y.C., Hu, S.C. and Lin, C.H. (2010). Effects of the Removal of 0.1 μm Particles in Industrial Cleanrooms with a Fan Dry Coil Unit (FDCU) Return System. *Aerosol Air Qual. Res.* 10: 571–580.
- Liu, B.Y.H., Romay, F.J., Dick, W.D. Woo, K.S., and Chiruta, M. (2010). A Wide-Range Particle Spectrometer for Aerosol Measurement from 0.010 μm to 10 μm . *Aerosol Air Qual. Res.* 10: 125–139.
- Makita, T., Nakamura, K., Tachibana, A., Masusaki, H., Matsumoto, K. and Ishihara, Y. (2003). Quantum Chemical Mechanism of Heterogeneous Reaction

- Between Trichlorosilane and Adsorbed Water. *Jpn. J. Appl. Phys.* 42: 4540–4541.
- Mores, T.F. (1984). *Fundamental Studies of Laser Interaction in Materials Preparation: New Aspects of Chemical Vapor Deposition, Trichlorosilane, Literature Survey and Combustion Experiments*, DTIC, USA.
- Ning, Z., Sioutas, C. (2010) Atmospheric Processes Influencing Aerosols Generated by Combustion and the Inference of Their Impact on Public Exposure: A Review, *Aerosol Air Qual. Res.* 10: 43–58.
- Rabinowitz, P.M. and Siegel, M.D. (2002). Acute Inhalation Injury. *Clin. Chest Med.* 23: 707.
- Ramachandran, G. (2005). *Occupational Exposure Assessment for Air Contaminants*, CRC Press, Taylor & Francis Group, New York, USA.
- Salem, S.A.K. H. (2005). *Inhalation Toxicology*, 2nd ed., CRC Press, Taylor & Francis Group, New York, USA.
- Schenkel, A. and Schaber, K. (1995). Growth of Salt and Acid Aerosol-particles in Humid Air. *J. Aerosol Sci.* 26: 1029–1039.
- Shih, T.S., Shih, M., Lee, W.J., Huang, S.L., Wang, L.C., Chen, Y.C., and Tsai, P.J. (2009) Particle Size Distributions and Health-related Exposures of Polychlorinated Dibenzo-p-dioxins and Ddibenzofurans (PCDD/Fs) of Sinter Plant Workers. *Chemosphere* 74: 1463–1470.
- Shih, Y.C., Hu, S.C., Ku, C.W. and Chein R. (2010). Particle Deposition on a 300 mm Wafer Moving in the Opposite Direction of the Airflow in a Uni-directional Cleanroom. *Aerosol Air Qual. Res.* 10: 316–322.
- Shiue A., Hu S.C. and Tu M.L. (2010). Particles Removal by Negative Ionic Air Purifier in Cleanroom. *Aerosol Air Qual. Res.* 11: 179–186.
- Tsai, P.J., Vincent, J.H. and Mark, D. (1996). Semi-empirical Model for the Aspiration Efficiencies of Personal Aerosol Samplers of the Type Widely Used in the Occupational Hygiene. *Ann. Occup. Hyg.* 40: 93–113.
- Tsai, P.J., Vincent, J.H., Mark, D. and Maldonado, G. (1995). Impaction Model for the Aspiration Efficiencies of Aerosol Samplers in Moving Air under Orientation-Averaged Conditions. *Aerosol Sci. Technol.* 22: 71–286.
- Uyan, Z., Carraro, S., Piacentini, G. and Baraldi E. (2009). Swimming Pool, Respiratory Health, and Childhood Asthma: Should we Change our Beliefs. *Pediatr. Pulmonol.* 44: 31–37.
- Vincent, J.H. (2005). Health-related Aerosol Measurement: A Review of Existing Sampling Criteria and Proposals for New Ones. *J. Environ. Monit.* 7: 1037–1053.
- Williams, E. (2000). Global Production Chains and Sustainability, In *The Case of High-purity Silicon and its Applications in IT and Renewable Energy*, United Nation University, Tokyo, Japan

Received for review, March 15, 2011

Accepted, April 18, 2011